

University of Texas at Arlington

**MavMatrix**

---

2019 Spring Honors Capstone Projects

Honors College

---

5-1-2019

## CHARACTERIZATION OF SCLERACTINIAN CORAL CASPASES IN COMPARISON WITH HUMAN HOMOLOGS

Jessica Lynn Tung

Follow this and additional works at: [https://mavmatrix.uta.edu/honors\\_spring2019](https://mavmatrix.uta.edu/honors_spring2019)

---

### Recommended Citation

Lynn Tung, Jessica, "CHARACTERIZATION OF SCLERACTINIAN CORAL CASPASES IN COMPARISON WITH HUMAN HOMOLOGS" (2019). *2019 Spring Honors Capstone Projects*. 28.  
[https://mavmatrix.uta.edu/honors\\_spring2019/28](https://mavmatrix.uta.edu/honors_spring2019/28)

This Honors Thesis is brought to you for free and open access by the Honors College at MavMatrix. It has been accepted for inclusion in 2019 Spring Honors Capstone Projects by an authorized administrator of MavMatrix. For more information, please contact [leah.mccurdy@uta.edu](mailto:leah.mccurdy@uta.edu), [erica.rousseau@uta.edu](mailto:erica.rousseau@uta.edu), [vanessa.garrett@uta.edu](mailto:vanessa.garrett@uta.edu).

Copyright © by Jessica Lynn Tung 2019

All Rights Reserved

CHARACTERIZATION OF SCLERACTINIAN  
CORAL CASPASES IN COMPARISON  
WITH HUMAN HOMOLOGS

by

JESSICA LYNN TUNG

Presented to the Faculty of the Honors College of  
The University of Texas at Arlington in Partial Fulfillment  
of the Requirements  
for the Degree of

HONORS BACHELOR OF SCIENCE IN BIOLOGY

THE UNIVERSITY OF TEXAS AT ARLINGTON

May 2019

## ACKNOWLEDGMENTS

First and foremost, I would like to thank my principal investigator Dr. Clay Clark for his mentorship and the opportunity to work in his lab. Dr. Clark has been instrumental in developing my interest in biochemical research, and I am fortunate to have stumbled into a lab that so enthusiastically invests time and resources into their undergraduate students.

I would also like to acknowledge the help of my research superiors: Dr. Robert Grinshpon for recruiting me into the Clark lab and undertaking my training, Suman Shrestha for his guidance and collaboration on this project, and Liqi Yao for her encouragement and mutual love of ramen and milk tea. Everyone in the Clark lab family has made invaluable contributions to my research experience; they all have inspired me to continue probing into life's mysteries by pursuing a career in research.

Additionally, I would like to thank both the Department of Biology and the Honors College of the University of Texas at Arlington for providing a positive, rigorous learning environment.

I would like to express my gratitude to my family for their undying support throughout my undergraduate career. Special thanks to my brother, Wesley Tung, for his words of wisdom about school and life beyond. Words cannot describe how thankful I am for our late-night Skype study sessions, despite the 900 miles between our universities. I am grateful for my sister (and best friend), Emily Tung, whose daily phone calls brought much needed sisterly fun and nonsense. Most importantly, I could not have weathered the

many storms of the last few years without my mother, Maggie Chen. None of my achievements would have been possible without her love, encouragement, and faith.

Last but not least, I would like to thank my cat, Saber, for her constant and loyal companionship. I spent many late nights writing this thesis with a cup of coffee in hand and Saber napping at my feet.

November 15, 2018

## ABSTRACT

### CHARACTERIZATION OF SCLERACTINIAN CORAL CASPASES IN COMPARISON WITH HUMAN HOMOLOGS

Jessica Lynn Tung, B.S. Biology

The University of Texas at Arlington, 2019

Faculty Mentor: Allan Clay Clark

Coral bleaching is an immune response where compromised algal symbionts are expelled from host tissue. *Porites astreoides* and *Orbicella faveolata* are model species on opposing ends of the immunity spectrum. Disease-resistant *P. astreoides* employs adaptive autophagic mechanisms when immunocompromised, while disease-sensitive *O. faveolata* activates caspase-mediated apoptosis. Presented here is a characterization of caspase homologs found in disease-tolerant *P. astreoides* (P.ast-3, P.ast-7) and disease-susceptible *P. astreoides* (O.fav-3a, O.fav-3b). P.ast-7 and O.fav-3a are unusual in that they retain high sequence similarity to human executioner caspases but possess a CARD-like domain characteristic of initiator and inflammatory caspases. Results indicate that P.ast-7 and O.fav-3a are monomers preferring aspartate in the P1 substrate position, corroborated by low activity against canonical caspase substrate Ac-DEVD-AFC. O.fav-3b and P.ast-3 are

dimers preferring valine in P1, but inactivity against Ac-VEID-AFC suggests additional specificity. A crystal structure of P.ast-7 bound with DEVD-CHO reveals two potential regulatory sites: first, a unique insertion of RYP residues was found to form hydrogen bonds with the substrate, and second, an N-terminal peptide bound near the active site is hypothesized to serve as an exosite. This study of basal metazoan caspases is pertinent to understanding the phenomenon of coral bleaching, as well as the evolution of human caspase substrate specificity and regulatory mechanisms.

## TABLE OF CONTENTS

ACKNOWLEDGMENTS .....	iii
ABSTRACT.....	v
LIST OF ILLUSTRATIONS.....	ix
LIST OF TABLES .....	x
Chapter	
1. INTRODUCTION .....	1
2. LITERATURE REVIEW .....	7
2.1 Consequences of Disrupted Symbiosis: Coral Bleaching.....	7
2.2 Caspase-Mediated Apoptosis in Coral.....	8
3. MATERIAL AND METHODS.....	13
3.1 Protein Purification .....	13
3.1.1 Purification Buffer Guide .....	14
3.2 Substrate Phage Display .....	14
3.2.1 Substrate Phage Display Buffer Guide .....	15
3.3 Fluorometric Enzyme Assays .....	15
3.4 X-ray Crystallography .....	16
4. RESULTS .....	18
4.1 Protein Purification.....	18



4.2 Substrate Phage Display and Fluorometric Enzyme Assays .....	19
4.3 Resolved Crystal Structure of P.ast-7 .....	21
5. DISCUSSION.....	26
REFERENCES .....	29
BIOGRAPHICAL INFORMATION.....	37

## LIST OF ILLUSTRATIONS

Figure	Page
1.1 Qualitative Difference Between Bleached vs. Healthy Coral.....	2
1.2 Working Model of Coral Disease Resistance .....	3
1.3 Multiple Sequence Alignment of Coral and Human Executioner Caspases .....	5
1.4 Inactive Human Executioner Caspase-7 Zymogen.....	5
1.5 Domain Organization of Coral Caspases .....	6
1.6 Intrinsic Activation Human Initiator Caspase-9 .....	6
3.1 General Principles of Substrate Phage Display .....	15
4.1 SDS-PAGE Gel of Purified Coral Proteins .....	19
4.2 Results of Substrate Phage Display Experiments .....	19
4.3 Fluorometric Enzyme Assay Data (Michaelis-Menten Curves).....	21
4.4 Crystallized P.ast-7 + DEVD-CHO .....	22
4.5 Resolved P.ast-7 Structure .....	23
4.6 P.ast-7 Active Site Bound with DEVD-CHO inhibitor .....	24
4.7 Hydrogen-Bonding Network of DEVD-CHO in the Active Site .....	24
4.8 Interaction of P.ast-7 RYP Residues with DEVD-CHO.....	25
4.9 Extra N-Terminal Bound Peptide with Electron Density .....	25

## LIST OF TABLES

Table		Page
3.1	Activity Assay Experimental Set-Up .....	16
4.1	Activity Assay Results: $k_{cat}/K_M$ values ( $M^{-1}s^{-1}$ ) .....	20
4.2	Crystallography Statistics for Resolved P.ast-7 Structure.....	22

## CHAPTER 1

### INTRODUCTION

Coral reefs are an irreplaceable bedrock of marine diversity, and coral mortality is closely linked to climate change. Rising seawater temperatures upset the symbiosis between reef-building cnidarians and photosynthetic algae (zooxanthellae). In this evolutionarily-ancient partnership, the zooxanthellae fix carbon and recycle nitrogenous waste for their coral hosts in return for a light-exposed, intracellular refuge. The breakdown of this relationship is a phenomenon known as coral bleaching, where coral hosts expel their algal symbionts in response to environmental stressors. The resulting animal has a “bleached” appearance, as the vibrant coloration of ocean reefs is attributed to the photosynthetic pigments found in zooxanthellae (Burkepile & Haye, 2008). The physiological mechanism behind bleaching is still not well understood; The Oxidative Theory of Coral Bleaching suggests that under environmental stress, algal symbionts overproduce reactive oxygen species (ROS) that threatens intracellular components of their host (Downs et al., 2002). According to this theory, the expulsion of symbionts is considered an immune response to this cellular threat. However, there is conflicting evidence over whether oxidative stress is the casual effect of algal expulsion or a late-stage response to the bleaching process (Tjus et al., 2001; Warner, Fitt, & Schmidt, 1999; Lesser, 1997; Nielsen, Petrou, & Gates, 2018).

Given sufficient time and severity, a bleached coral will starve and die. However, bleaching is not an irreversible process, and different species of coral have demonstrated

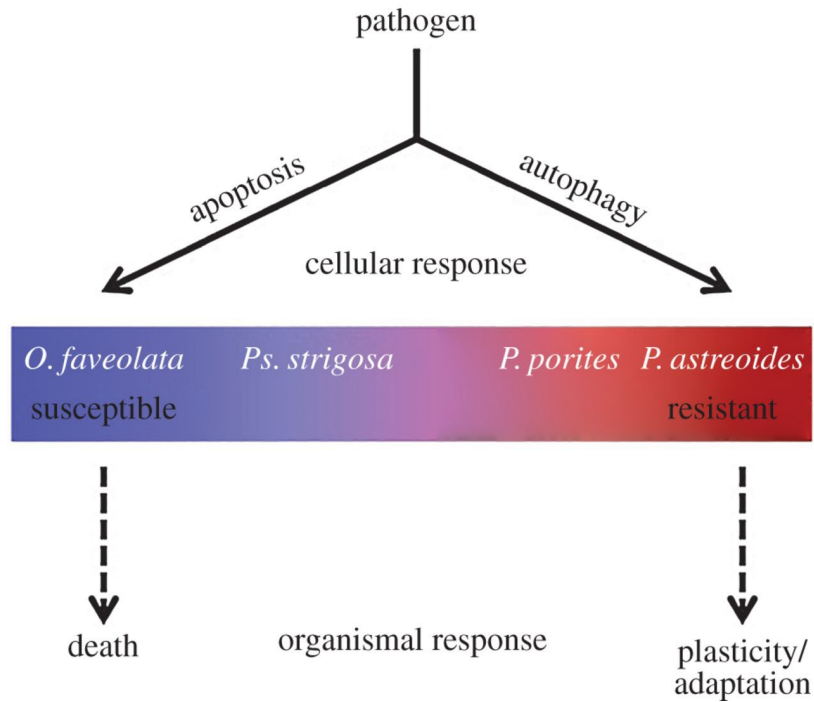
variable rates of algal recovery (Marshall & Baird, 2000). There is considerable incentive to elucidate the characteristics responsible for this difference in survivability potential post-bleaching. Recent trends show that mass bleaching events are increasing in scale and frequency (De'ath et al., 2012; Sutherland, Porter, & Torres, 2004). Significant conservation efforts are needed to ensure the continuing existence of marine reefs, as they are both a critical habitat for much of the ocean's biodiversity and a vital resource for human agriculture and industry.



Figure 1.1: Qualitative Difference Between Bleached vs. Healthy Coral  
Right: a specimen of bleached *O. faveolata*. Left: a specimen of healthy *P. astreoides*.

In 2017, a study done by Fuess et al. revealed a correlation between the sensitivity of a coral and the cellular mechanism it activates following an immune challenge. Sensitive species of coral, like *Orbicella faveolata*, were found to activate apoptotic cell death, whereas hardier species, like *Porites astreoides*, were found to activate an adaptive autophagic response (Fig 1.2). Furthermore, disease-susceptible species were found to elicit higher levels of caspase activity following immune stimulation. These findings suggest that the downregulation of apoptotic genes may increase stress tolerance, and upregulation of apoptotic genes may exacerbate stress sensitivity. Investigation of

cnidarian cell death mechanisms appears to be key in defining a coral’s threshold of stress tolerance prior to bleaching.



**Figure 1.2: Working Model of Coral Disease Resistance**  
 Reprinted from “Life or death: disease-tolerant coral species activate autophagy following immune challenge.” by L. E. Fuess, E. Weil, R.D. Grinshpon, L.D. Mydlarz, 2017, Proceedings of the Royal Society B: Biological Sciences, 284(1856), 6. Copyright [2017] by L.D. Mydlarz. Reprinted with permission.

Caspases are a family of cysteine-aspartate specific proteases that are essential in facilitating apoptosis and cellular inflammation (Ramirez & Salvesen, 2018). The majority of caspase research has primarily focused on those found in vertebrates, where caspase dysfunction contributes to cancer and neurodegenerative conditions like Alzheimer’s disease and Huntington’s chorea (Renahan, Booth & Potten, 2001). Apoptosis was first characterized in *Caenorhabditis elegans* (Ellis & Horvitz, 1986) and later *Drosophila* (Song, McCall, & Steller, 1997); however, the apoptotic pathways of these model organisms are very different from that in mammals and do not appear to represent ancestral characteristics. In contrast, vertebrate apoptotic machinery appears to have retained many

characteristics found in sponges, sea anemone, and coral (Wiens et al., 2003; Tchernov et al., 2011; Richier et al., 2006). Caspases are potential targets for pharmacological modulation of cell death, but strong evolutionary conservation across the caspase family has hindered drug development (Mackenzie, Schipper, & Clark, 2008). The study of marine invertebrate caspases may shed light on the evolution of caspase substrate specificity and promote rational drug design.

Presented here is an initial characterization of four caspases found in *P. astreoides* and *O. faveolata*, species found on opposite ends of the stress-tolerance spectrum. The coral caspases were selected for their sequence similarity to human executioner caspases, which are the main effectors of apoptosis. An initial BLAST (Basic Local Alignment Search Tool) search showed that the two sequences from *P. astreoides* had high similarity to human caspase-3 and caspase-7. Therefore, they are denoted here as P.ast-3 and P.ast-7. The two sequences from *O. faveolata* both showed high similarity to human caspase-3, and as such are O.fav-3a and O.fav-3b. P.ast-7 and O.fav-3a both possess a long pro-domain that has roughly 37% similarity with the CARD-domain of human initiator caspase-9. The domain organization of these proteins is illustrated in Figure 1.5. Generally speaking, human initiator caspases are monomers that dimerize upon activation, and human executioner caspases are dimeric zymogens (Fig. 1.7) that require cleavage of the inter-subunit linker for activation. In the intrinsic apoptotic pathway, upstream dimerization and inter-subunit cleavage of monomeric caspase-9 via the apoptosome complex is necessary to active downstream executioner caspases-3, -6, and -7 (Fig 1.6) (Clark, 2016). Preliminary size exclusion chromatography data (not discussed here) suggests that P.ast-7 and O.fav-3a are monomers, while P.ast-3 and O.fav-3b are dimers. The objectives of this

study were to further characterize these coral caspases by using: substrate phage display to find substrate specificity, fluorometric enzyme assays to determine catalytic efficiency, and X-ray crystallography to solve structural models.

<b>caspase-6</b>	MSS-----ASG---
<b>caspase-3</b>	MEN-----TEN---
<b>Ofav3b</b>	MSS-----KFKIHV
<b>Past_casp3</b>	MS-----KFNITVV
<b>Ofav3a</b>	MEQSDRDILRKNRQDLLKDMEAKRVASRLYSRGIFSEEDKDEVNSKSTTNEQGECLLDLILPKRGPKAFRAFCDVLHELSPHLE--SLLRPVQEAGIP---
<b>Past_casp7</b>	MQEEDRKALRSNREALLKDLAKRVASLLYSREIFSEEDKDSVNAKSTFSEQREEVLDLILPKRGPKAFSAFCNVLHEVSPHLE--ALLRPIQE---D---
<b>caspase-7</b>	M-----ADDQGCIEEQGVDSANED---
<b>caspase-6</b>	-----LR-----RGHPAGG-----EENMTETDAF-----YKREMFDPAEKYKMDH--RRRGIALIFNHERFFWHIT--LPE-
<b>caspase-3</b>	-----SV-----DSKSIKN-----LEPKIIHGSES-----MDSGISLDNSYKMDY--PEMGLCIIINKNFHKSTG--MTS-
<b>Ofav3b</b>	ADCSGAVVI-----GDHANLTVEAPVAGAGPQRRPVREQ-----AAAATTSTHAPCQESSGDDINYKAKSGYVLVINNYIFPRRD---DVE-
<b>Past_casp3</b>	SGCAGNIVV-----GDHAVLNVGASSTDARPRKQPPSEE-----VPPTGPSQVH--CQESAGDGMNYIAKSGYVLVINNYLFPQRL---NVE-
<b>Ofav3a</b>	-----SEGTDG--GNKNPISS-----TSNLGASESADE--ADAKLFGFGGGSASAK---PSSSTLDKEIIYKMDR--STRGIAVIINKNFLRSSGM <b>RYP</b>
<b>Past_casp7</b>	-----DEGIDGPGSTAPIPA---SGV--PSENNDQ--ADAKLFSFGGGSAAK---SSANTIDNDTIYKMNK--STRGIAVIINNKDFLRSSGM <b>RYP</b>
<b>caspase-7</b>	-----SV-----DAKPRS---SFVPSLFSKKKKNVTMR-----SIKTRDRVPTYQYNNMF--EKLKGCIIINKNFKDKVTG--MGV-
<b>caspase-6</b>	RRGTCADRDNLTRRFSDLGFVEKCFNDLKAPELLKIHEVSTVSHADADCFVCFVLS <b>H</b> EGNHIYAYDA-KIEIQTLTGLFKGDKCHSLVKGPKFI IQA
<b>caspase-3</b>	RSGETDVAANLRETFRNLYEVRNKNDLTREEIVELMRDVSKEDEHSKRSSFVCVLLS <b>H</b> GEEGIIFGTNG--FVDLKKITNFFRGDRCSRSLTGKPKLFI IQA
<b>Ofav3b</b>	RTGSNDDVRNLTSLFDDFNFRHVVEDNQTSQMIKLLQTAEKDFSRDYFCVVCVILS <b>H</b> GKKGDIYGTDEELIKIEAITSLFRRNECPSELEGKPKFI LQA
<b>Past_casp3</b>	RTGSNDDVKNLTNLFDDFGFRSRVQDNQTRSEMLSLKDTAEKDFSKYDCVFCVILS <b>H</b> GSKDGIYGTDEVINIEAITSLFRRDECPSELEGKPKFI LQA
<b>Ofav3a</b>	RNGTDVDRDSLVLKFRMLKFEVKIYNDRTKAEIRITIKEMATLNHSNYDAFIFSLIL <b>H</b> GEEGVIYGTDG--TISRDLTAEFK--YSTSLAGKPKLFFPQA
<b>Past_casp7</b>	RNGTDVDRDALAKLFRALKFDVRIYNNQTRAEIRITIKEMAITNHPTPYDAFIFSLIL <b>H</b> GEEGVIYGTDG--TMAIKDLTAIFK--DCTTLVKGPKMFFPQA
<b>caspase-7</b>	RNGTDKDAEALFKCFRSLGFDVIVYNDSCARKQDLKKASEEDHTNAACFACILL <b>S</b> SEENVIYKDG--VTPIKDLTAHFRGRDRCTLLEKPKLFFIQA
<b>caspase-6</b>	<b>C</b> RGN-QHDVPIPLDVVDNQTEKLDNTNITEVDAASVYTLPGADFLMCSVAEGYSHRETVNGSWYIQDLCEMLG--KYGSSLEFTELLTLVNRKV--SQR
<b>caspase-3</b>	<b>C</b> RGT-ELDCGIETDSGVD-----DDMACHKIPVEADFLYAYSTAPGYYSWRNSKDGSWFIQSLCAMLK--QYADKLEFMHILTRVNRKV--ATE
<b>Ofav3b</b>	<b>C</b> RGS-RRDITVPVESDSDP-----IPLSSSLPADADFLICFASAPDHESYRQAHLGSWFISSVVDVFK--EYAEERHLMMLLRVNNHV--AGF
<b>Past_casp3</b>	<b>C</b> RGN-QRDIVPVESDSDP-----MVFSNPSPADADFLICFASAPGHQSYRQPLLGSWFISAVFDVFK--EHAEREHIMDMMLRVNNQV--AGY
<b>Ofav3a</b>	<b>C</b> QH-EYMDGMDVTDAP-----QENKVSVPAAEDFLYAYSTVPGYYSWRNSVNGSWFIQSLTKVFE--DNAERMDILRMLTRVNAMV--STY
<b>Past_casp7</b>	<b>C</b> QH-EYMDGMDVTDAP-----QQGSKVSPAAEDFVYAYSTVPGYYSWRNSVNGSWFIQSLTKVFE--ENAERMDILRMLTRVNAMV--STY
<b>caspase-7</b>	<b>C</b> RGT-ELDDGIQADSGPIN-----DTDANPRYKIPVEADFLFAYSTVPGYYSWRSPGRGSWFQALCSILE--EHGKDLIMQILTRVNRV--ARH
<b>caspase-6</b>	RVDFCKDP--SAIGKKQVPCFASMLTKKLHFFPKSN----
<b>caspase-3</b>	FESFSFDA--TFHAKKQIPCIVSMLTKELYFYH-----
<b>Ofav3b</b>	YSK-----EGLKQIPQCVMCRKKVFFDPKYS----
<b>Past_casp3</b>	YSR-----DGLKQMPQCICMLTKKVFQPRYGSS--
<b>Ofav3a</b>	KSR--TGDY--YSDSKRQVSSIVSMLRKELYFFPENVEQS--
<b>Past_casp7</b>	KSR--TGDY--YSDSKRQVSSVVSMLRKELYFFPENVTQS--
<b>caspase-7</b>	FESQSDDP--HFHEKKQIPCVSMLTKELYFSQ-----

Figure 1.3: Multiple Sequence Alignment of Coral and Human Executioner Caspases  
 Boxed in green: unique RYP insertion. Boxed in blue and red are the catalytic cysteine-histidine dyad.

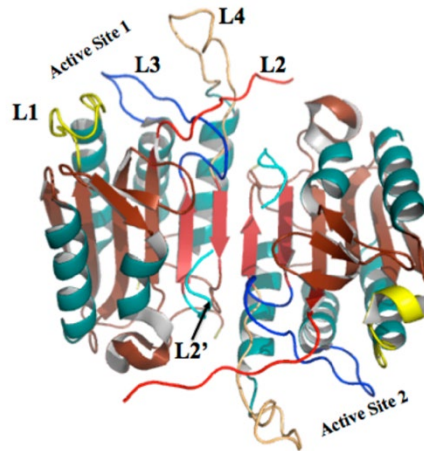


Figure 1.4: Inactive Human Executioner Caspase-7 Zymogen

Caspases have four active site loops, L1 – L4 that originate from one monomer, and one loop, L2', that originates from the second monomer. *Reprinted from "Caspase Allosteric and Conformational Selection," by A.C. Clark, 2016, Chemical Reviews, 116(11), 6692.*





**Figure 1.5: Domain Organization of Coral Caspases**

Orange: CARD motif characteristic of human initiator caspases-2 and -9.

Purple: Large subunit. Blue: small subunit. Inter-subunit linker is represented by the grey section between the large and small subunits.

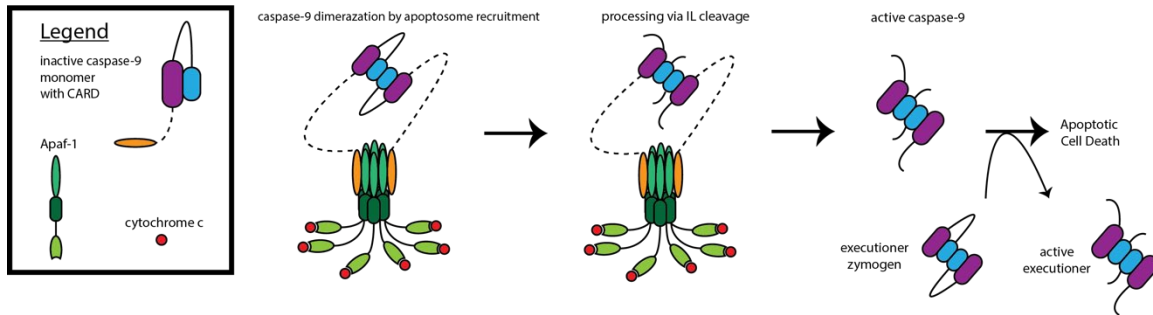


**Figure 1.6: Intrinsic Activation of Human Initiator Caspase-9**

Dimerization and IL-processing via CARD-CARD recruitment by the apoptosome.

The executioner caspases undergo IL-processing by the active caspase-9.

## CHAPTER 2

### LITERATURE REVIEW

#### 2.1 Consequences of Disrupted Symbiosis: Coral Bleaching

The decline of coral reef ecosystems has coincided with the onset of anthropogenic climate change. These profoundly devastating, arguably permanent, alterations to the most biodiverse of marine landscapes are direct consequences of human industry—the most notable culprits being deforestation and fossil fuel consumption. Both of these practices contribute to rising seawater temperatures by releasing excessive amounts of greenhouse gases (in the forms of CO<sub>2</sub> and CH<sub>4</sub>) into the atmosphere, where they effectively trap thermal energy radiating from the sun (Hughes, 2003). One of the model ecosystems used to study the impact of climate change on marine environments is the Great Barrier Reef, which is the world's largest coral reef found off the northeastern coast of Australia (De'ath et al., 2012). Scleractinian corals have a mutualistic relationship with photosynthetic zooxanthellae (of genus *Symbiodinium*) that dates back to the Triassic Period 240 million years ago. This endosymbiosis, in which the zooxanthellae (algae) provide the host with sustenance through photosynthesis and recycling of nitrogenous waste, was established early on in coral evolution and was likely the driving force behind its ecological success in nutritionally deficient waters (Frankowiak, 2016). Reef-building corals are sensitive to temperature change, and under adverse conditions are known to expel algal symbionts from host tissue in a phenomenon called coral bleaching. Because these algal symbionts are responsible for about 90% of the coral's metabolic needs, the mortality rates of bleached

corals unable to recover their symbionts are high (Burriesci, Raab & Pringle, 2012; Oakley & Davy, 2018).

Mass bleaching events have been well-documented since the 1980's (Hughes et al., 2018), and long-term studies of the Great Barrier Reef, the world's largest coral reef found off the northeastern coast of Australia, show consistent losses in coral cover over the last three decades (De'ath et al., 2012). Studies of Caribbean and Indo-Pacific reefs have reported similar or even higher statistics, although these areas also experience high-disease prevalence that exacerbates reef decline (Sutherland, Porter, & Torres, 2004). Other factors like ocean acidification (Erez et al., 2010), destructive fishing practices (McManus, 1997), and water pollution (Thurber, 2013) add additional hardships to marine reef recovery. Coral reefs are an invaluable site for ocean wildlife because they provide shelter for thousands of different aquatic species. The ecosystems that reefs cultivate are vital aspects of marine biodiversity, which in turn benefits human causes like coastline protection, the fishing industry, and drug discovery. The decline of reefs is an alarming threat to not only its immediate inhabitants but also the greater ecosystem that spans our oceans (Moberg & Folke, 1999).

## 2.2 Caspase-Mediated Apoptosis in Coral

Programmed cell death (PCD) is an umbrella term describing the many mechanisms of deliberate cell suicide. The evolutionary advent of multicellularity necessitated such systems of regulated cell turnover (Huettenbrenner et al., 2003). One form of PCD is apoptosis, a critical genetically-encoded physiological pathway that balances cell proliferation with cell deletion. Apoptosis is induced in a cell after it crosses a certain threshold of dysfunction, like extensive DNA damage or high levels of ROS production,

which allows compromised cells to self-destruct in order to protect neighboring cells. This process is also essential for driving organismal development and maintaining homeostasis. For example, apoptotic regulation plays a role in shaping individual fingers and toes during intrauterine growth. Apoptotic dysfunction has been implicated in both neurodegenerative conditions like Alzheimer's disease (excess cell death) and cancer (deficient cell death) (Lemasters, 2009). Apoptotic cells display very distinct changes in morphology, including membrane blebbing, cell shrinkage, chromatin condensation, and DNA fragmentation. Formation of apoptotic bodies through membrane blebbing isolates the intracellular contents from the environment, which surrounding cells can uptake through phagocytosis (Kerr, Wyllie, & Currie, 1972).

Apoptosis is carried out by a family of evolutionarily-conserved enzymes known as caspases, or cysteinyl-aspartate-specific proteases. Caspases are homodimers of protomers, and each protomer is composed of a large and small subunit connected by an inter-subunit linker. An active caspase homodimer has two active sites, each formed by the four mobile loops of one protomer (L1-L4) and one loop from the second protomer (L2'). Upon dimerization, each protomer is oriented so that the large subunits face outward while the small subunits make contact at the dimer interface. All caspases use a catalytic cysteine-histidine dyad to cleave a tetra-peptide substrate (N'-P4-P3-P2-P1-C') between the P1 and C-terminus. Caspases are unique among proteases because they demonstrate an absolute requirement for aspartate in the P1 substrate position but have variable specificities for the P2-P4 positions (Ramirez & Salvesen, 2018). Research efforts have primarily centered around the 11 human caspases, which can be grouped by residue preference in the P4 position. Group I (caspases-1, -4, -5, -14) prefers bulky amino acids like tryptophan or

leucine ((W/L)EHD); Group II (caspases-2, -3, -4) prefers charged amino acids like aspartate (DEXD); Group III (caspases-6, -8, -9, -10) prefers aliphatic hydrophobic amino acids like leucine, isoleucine, or valine ((L/I/V)EXD). X refers to a position that allows for different amino acids (Clark, 2016).

The human caspases are also classified by their role in the apoptotic caspase cascade (Boatright & Salvesen, 2003). Initiator caspases (-2, -8, -9, -10) are monomers activated upstream of executioner caspases (-3, -6, -7). Initiators have long pro-domains that contain one of two regulatory recruitment motifs: the death effector domain (DED) that receives extracellular (extrinsic) apoptotic signals, or the caspase recruitment domain (CARD) that receives intracellular (intrinsic) apoptotic signals. The extrinsic pathway proceeds through ligand-binding to a transmembrane receptor, which stimulates the formation of a death-inducing signaling complex (DISC) that recruits the DED domain of initiators caspase-8 and -10. In the intrinsic pathway, pro-apoptotic proteins like BAX and BAK increase the permeability of the outer mitochondrial membrane (Wei et al., 2001). The cytochrome C released from the intermembrane space binds to Apaf-1 (Apoptotic protease activating factor-1), where it further oligomerizes into a wheel-shaped complex called the apoptosome. The apoptosome is the recruiting platform for inactive initiator caspase-9 monomers, and dimerization and IL-cleavage proceed through CARD-CARD interactions. (Riedl & Salvesen, 2007). Caspase-2 is activated in a similar fashion, although its complex, the PIDDosome, is composed of the CARD-carrying proteins RAIDD and PIDD1. Caspase-2 does not require IL-cleavage for activation (Jang & Park, 2013; Tinel, 2004).

Executioner procaspases-3, -6, and -7 exist as stable homodimers that become active upon IL cleavage by an initiator caspase. Before IL cleavage, the dimerized zymogen demonstrates little substrate affinity due to poor positioning of the two active sites. The substrate binding pockets becomes properly aligned upon IL processing. Executioner caspases carry out apoptosis by degrading critical structural elements of the cell and activating other proteins with similar catabolic functions (Mackenzie & Clark, 2012).

Caspases present a challenge to drug discovery because they have evolved discrete regulatory mechanisms while retaining high active site structural similarity (Clark, 2016). Consequently, drugs targeting the caspase active site may have high degrees of cross-reactivity among other caspase family members. (Mackenzie, Schipper, & Clark, 2008). For this reason, the field of evolutionary biochemistry has taken an interest in the caspase family. This inter-disciplinary method of studying the protein structure-function relationship may shed light on how the caspases have differentiated over time. The oldest caspase ancestor, known as the 'meta-caspase,' evolved before the rise of multicellularity; caspases are therefore ubiquitous across eukaryotic phylogenies (Huettenbrenner et al., 2003), including basal metazoans like sponges, sea anemone, and coral (Wiens et al., 2003; Richier et al., 2006; Tchernov et al., 2011). A study published in 2004 found that elevated temperatures induce high-frequency, early-onset apoptosis in *Aiptasia pallida* endoderm, which is where algal symbionts reside (Dunn et al. 2004). Later, a caspase found in *A. pallida* was reported to have attributes of both human initiator and executioner caspases (Dunn et al., 2006). Heat-induced apoptosis has been correlated with the relative upregulation of the anti-apoptotic protein Bcl-2 in the coral *Acropora millepora*; their results indicate a delayed decrease in the apoptotic activity of surviving cells, suggesting

that corals may possess regulatory mechanisms to compensate for sudden environmental changes (Pernice et al., 2011). Additionally, caspase-3-like activity has been detected in the stony coral *Pocillopora damicornis* when exposed to heat-stress and high levels of ammonium (Yu et al., 2017); application of universal caspase inhibitors been shown to prevent the death of bleached coral (Tchernov et al., 2011). In 2017, Fuess et al. found that sensitive corals, like *O. faveolata*, activate caspase-mediated apoptosis in the face of an immune challenge, while hardier corals, like *P. astreoides*, activate adaptive autophagic mechanisms. Their results suggest a model in which the compensatory pathway selected dictates the coral's overall tolerance to stress and disease.

## CHAPTER 3

### MATERIAL AND METHODS

Protocol adapted from Grinshpon, 2018 and Fuess et al., 2017

#### 3.1 Protein Purification

Each coral caspase gene (modified to include a tag of 6 histidine residues) was transformed into BL21 pLysS *E. coli* cells using a pET-11a vector. The proteins were purified via immobilized metal ion affinity chromatography (IMAC) with HisPur™ Ni-NTA Resin. One-liter Fernbach flasks of Luria broth were spiked with an overnight *E. coli* culture to a starting OD<sub>600</sub> of 3 (0.3 for a 1:10 dilution). The temperature was lowered to 25°C as the OD<sub>600</sub> approached 1.2 (0.12 for a 1:10 dilution). Expression was induced with final [0.5 mM IPTG] for 4-5 hours. The cultures were then spun down at 5000 RPM for 10 minutes, and the collected pellets resuspended in 100 mL lysis buffer for 4 hours - overnight. Buffer pH is important in maintaining protein solubility, and the buffers used for the study are listed in the subsection below.

Equilibration of the IMAC column is necessary to first, chelate impurities from the resin, and second, charge the resin with nickel that will bind to each protein's histidine tag. One column of strip buffer was passed through the column, followed by a 1000 mL wash with diH<sub>2</sub>O. The resin was charged with 1/2 column of charge buffer, followed by 1/3 column of lysis buffer. After cell lysis via sonication, the samples were spun down at 14,000 RPM for 30 minutes. The collected supernatant was passed through the column as flow-through, and the resin washed with 300 mL of lysis buffer. The protein was eluted with



50 mL of elution buffer and dialyzed overnight. The flow-through, wash, and elution were run through an SDS-PAGE gel to verify the presence of the protein and to assess for impurities. Q-sepharose was used for further purification, if necessary.

### *3.1.1 Purification Buffer Guide*

Lysis buffer: 50 mM NaCl, 50 mM Tris, 50 mM Imidazole, pH 8.5

Strip buffer: 100 mM EDTA, pH 8.8

Charge buffer: 100 mM NiSO<sub>4</sub>

Elution buffer: 100 mM NaCl, 50 mM Tris, 500 mM Imidazole, pH 8.5

Dialysis buffer: 100 mM NaCl, 50 mM Tris, 500 mM Imidazole, pH 8.5

## 3.2 Substrate Phage Display

For substrate phage display experiments, two 100 µL samples (one control and one experiment) of an M13 phage library (XXXXDX or XXXXXX) were bound to 150 µL Ni-NTA resin, along with 200 µL of blocking buffer for 30 minutes at room temperature. Unbound phage were washed away with blocking buffer, wash buffer, and activity buffer (solutions listed below). 5 µL of 10% CHAPS and 2.5 µL of 1 M DTT were then added to the samples, along with 10 µL of 2µM protein to initiate the reaction for 2-3 hours. ER-2738 *E. coli* strain cells were used to amplify the cleaved phage by infecting cells with the supernatant collected from the reaction. These cells were cultured for 4 hours, and the supernatant was used as the library for the next round of selection (Fig 3.1). Serial titer dilutions were plated on 2xYT agar plates with a lawn of ER-2738 cells in the presence of X-gal and IPTG to determine phage concentration in the experiment vs. control. The infected cells turned blue, and the plaques were picked for sequencing. The colonies were counted to determine the end of the experiment, which is when the amount of library bound

to the resin is equivalent to the amount cleaved during the reaction. Increased specificity was monitored by observing the amount of phage released during the experiment vs. control.

### 3.2.1 Substrate Phage Display Buffer Guide

Blocking buffer: 1 mg/mL BSA, 1X PBS, 1M NaCl, 0.1% Tween-80, 10 mM Imidazole

Wash buffer: 1X PBS, 1M NaCl, 0.1% Tween-80, 10 mM Imidazole

Elution buffer: 1 mg/mL BSA, 1X PBS, 1M NaCl, 0.1% Tween-80, 250 mM Imidazole

Activity buffer: 50 mM NaCl, 150 mM TRIS, 1% sucrose, pH 7.5

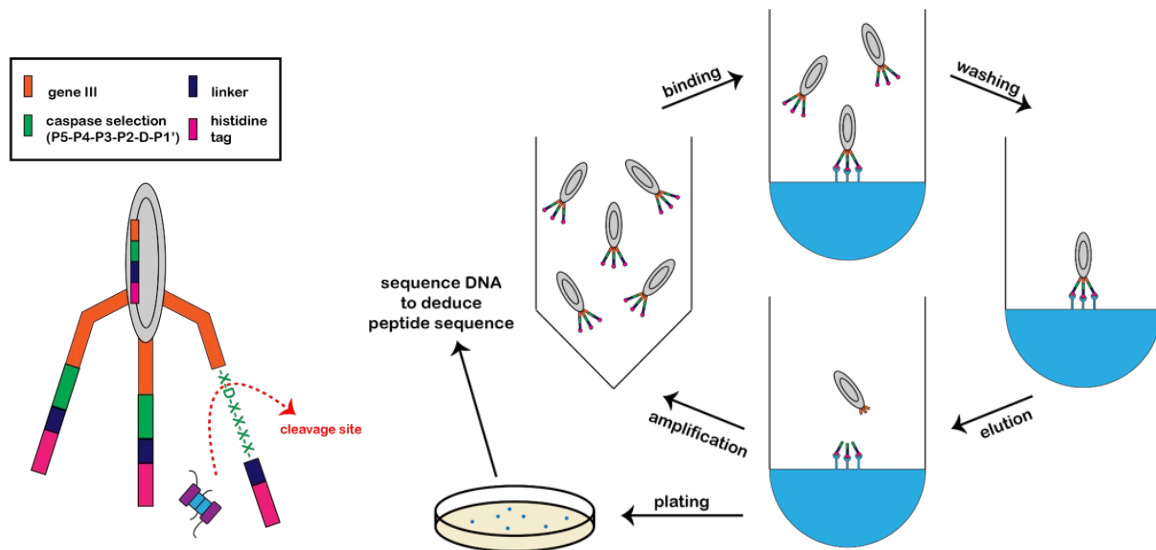


Figure 3.1: General Principles of Substrate Phage Display

Right: M13 phage and caspase cleavage site. Left: Substrate phage display protocol.

### 3.3 Fluorometric Enzyme Assays

The proteolytic activity of each caspase was measured in the presence of varying concentrations of substrates. This was done by using a PTI (Photon Technology International, Edison, NJ, USA) fluorometer to measure the generation of free AFC or AMC from different fluorogenic tetrapeptide substrates (Ac-DEVD-AFC, Ac-VEID-AFC,

Ac-LETD-AFC, Ac-LEHD-AMC, Ac-IETD-AMC) dissolved in DMSO. The excitation and emission wavelengths for samples using the AFC fluorophore 400 nm and 505 nm, respectively. The excitation and emission wavelengths for samples using the AMC fluorophore were 350 nm and 450 nm, respectively. A 200  $\mu\text{M}$  substrate stock was prepared using an activity buffer: [50 mM NaCl, 150 mM TRIS, 9% sucrose, pH 7.5]. The reactions were initiated by adding 20  $\mu\text{L}$  of a 0.1  $\mu\text{M}$  enzyme stock to 180  $\mu\text{L}$  of a reaction mixture (Table 3.1) for a 10 nM final enzyme concentration. The reaction mixture had a final volume of 200  $\mu\text{L}$ , including a final concentration of 10 mM DTT (Dithiothreitol) and 0.1% CHAPS (3-[(3-cholamidopropyl) dimethylammonio]-1-propanesulfonate). Substrate cleavage was monitored for 60 seconds. The amount of AFC cleaved during the reaction was determined by generating a standard curve of free AFC. Data was plotted in Kaleidagraph, and the steady-state parameters ( $k_{\text{cat}}$  and  $K_M$ ) were determined by fitting velocity vs. [substrate] with the Michaelis-Menten equation.

### 3.5 X-ray Crystallography

Table 3.1: Activity Assay Experimental Set-Up

[Substrate]	200 $\mu\text{M}$ Substrate Stock	10% CHAPS	1 M DTT	Activity Buffer	0.1 $\mu\text{M}$ Enzyme Stock
0 $\mu\text{M}$	0 $\mu\text{L}$	2 $\mu\text{L}$	2 $\mu\text{L}$	176 $\mu\text{L}$	20 $\mu\text{L}$
5 $\mu\text{M}$	5 $\mu\text{L}$	2 $\mu\text{L}$	2 $\mu\text{L}$	171 $\mu\text{L}$	20 $\mu\text{L}$
10 $\mu\text{M}$	10 $\mu\text{L}$	2 $\mu\text{L}$	2 $\mu\text{L}$	166 $\mu\text{L}$	20 $\mu\text{L}$
20 $\mu\text{M}$	20 $\mu\text{L}$	2 $\mu\text{L}$	2 $\mu\text{L}$	156 $\mu\text{L}$	20 $\mu\text{L}$
30 $\mu\text{M}$	30 $\mu\text{L}$	2 $\mu\text{L}$	2 $\mu\text{L}$	146 $\mu\text{L}$	20 $\mu\text{L}$
45 $\mu\text{M}$	45 $\mu\text{L}$	2 $\mu\text{L}$	2 $\mu\text{L}$	131 $\mu\text{L}$	20 $\mu\text{L}$
60 $\mu\text{M}$	60 $\mu\text{L}$	2 $\mu\text{L}$	2 $\mu\text{L}$	116 $\mu\text{L}$	20 $\mu\text{L}$
75 $\mu\text{M}$	75 $\mu\text{L}$	2 $\mu\text{L}$	2 $\mu\text{L}$	101 $\mu\text{L}$	20 $\mu\text{L}$
100 $\mu\text{M}$	100 $\mu\text{L}$	2 $\mu\text{L}$	2 $\mu\text{L}$	76 $\mu\text{L}$	20 $\mu\text{L}$

X-ray crystallography requires purified protein samples concentrated to 8-10 mg/mL, stored at -80°C until needed. The protein sample was incubated with various inhibitors (0.01 M DEVD-CHO, IETD-CHO, or VEID-CHO in DMSO) on ice for 1 hour. Crystals were grown at 18°C using the hanging drop vapor diffusion method. Hampton crystal screens were used to find initial crystallization conditions. Each well contained 490 µL of the screen, 5 µL of 1 M DTT, 5 µL of 300 mM NaN<sub>3</sub>. Each drop contained 2 µL protein and 2 µL well solution. The screens of initial hits were refined. Crystals were flash frozen in liquid nitrogen (-196°C) with cryoprotectant and shipped to the SER-CAT synchrotron beamline in Argonne, IL.

## CHAPTER 4

### RESULTS

#### 4.1 Protein Purification

The purification protocol described in Chapter 3 was used to purify each of the coral caspases to varying degrees of success. High yields of P.ast-7, P.ast-3, and O.fav-3b were attained after IMAC chromatography, and these protein samples were subsequently run through a Q-sepharose column to remove any remaining impurities. O.fav-3a did not express well under these conditions, and no significant improvement was observed when the expression time was extended overnight with the final concentration of IPTG lowered to 0.2 mM. Very little protein was recovered as a result, and Q-sepharose was not pursued for this sample because the risk of total product loss is high with such low yields. However, enough O.fav-3a was recovered in a 6-liter purification for substrate phage display and activity assays; a larger volume of culture or different buffer conditions may be necessary to obtain samples of sufficient purity at crystallography concentration. Fig 4.1 show the SDS-page gels of each protein post-purification. The samples were concentrated with a centrifugal filter concentrator and aliquoted appropriately for later experiments. The concentration of protein was calculated using Beer's law:  $\text{Absorbance @ 280 nm} = \epsilon lc$ , where  $\epsilon$  is the molar extinction coefficient,  $l$  is the pathlength, and  $c$  is the concentration in mg/mL. The aliquots were stored at  $-80^{\circ}\text{C}$  until needed.

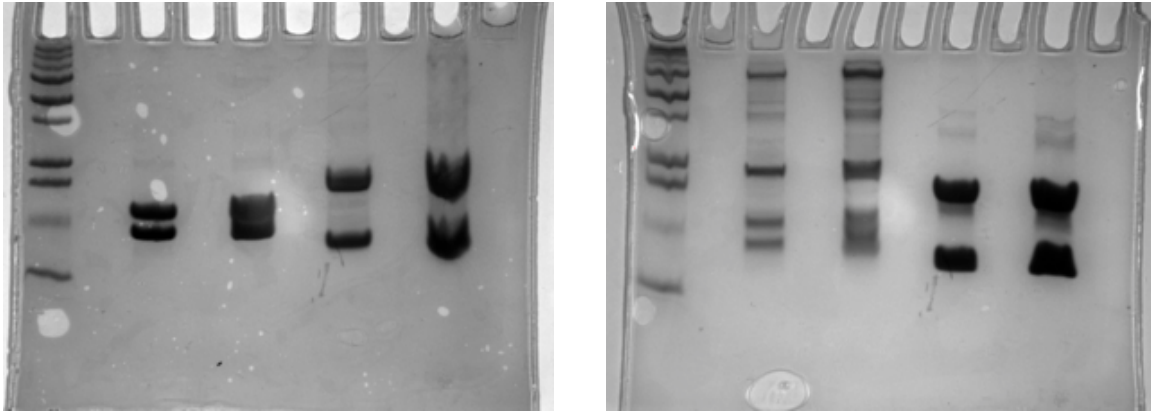


Figure 4.1: SDS-PAGE Gel of Purified Coral Proteins  
 Left (from left to right): ladder, 10 µL P.ast-7, 20 µL P.ast-7, 10 µL P.ast-3, 20 µL P.ast-3.  
 Right: ladder, 10 µL O.fav-3a, 20 µL O.fav-3a, 10 µL O.fav-3b, 20 µL O.fav-3b

#### 4.2 Substrate Phage Display and Fluorometric Enzyme Assays

Four rounds of substrate phage display were carried out for each protein before the amount of phage cleaved in the experiment was roughly equal to the amount eluted. This was repeated for both the XXXXXX and XXXDX phage library. The cleaved phage were re-plated on a lawn of ER-2738 *E. coli* cells and individual plaques were plated for DNA sequencing. Results showed that P.ast-7 and O.fav-3a have a Group II specificity for aspartate in the P4 position, while a Group III specificity for valine is found in P.ast-3 and O.fav-3b (Fig 4.2).

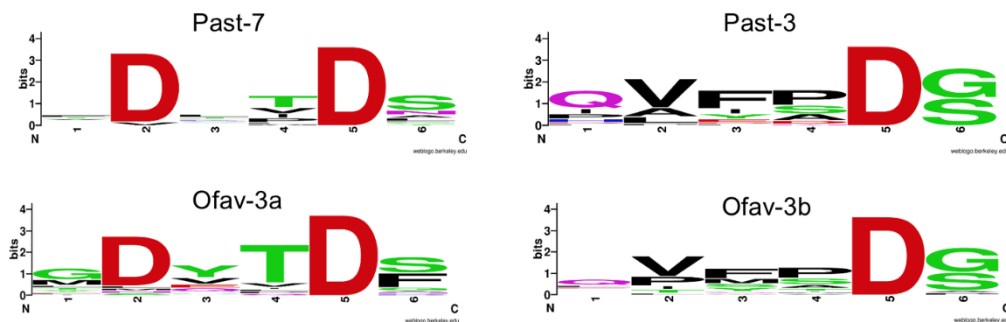


Figure 4.2: Results of Substrate Phage Display Experiments  
 Substrate positions from left to right: P5 – P4 – P3 – P2 – P1 – P1'. Note the fixed aspartate (D) at P1.

The P.ast-7 and O.fav-3a aspartate preference was corroborated by activity against canonical human caspase-3 substrate Ac-DEVD-AFC; however, the calculated  $k_{cat}/K_M$  values (Table 4.1) are not an accurate measure of the catalytic efficiency of these two proteins. Both P.ast-7 and O.fav-3a display a near-linear relationship between the reaction rate vs. [substrate], which is reflective of their high  $K_M$  values, the [substrate] at  $\frac{1}{2} V_{max}$  (Fig 4.3). These  $k_{cat}/K_M$  values were generated by fitting the Michaelis-Menten equation to data that was collected below our equipment's threshold of detection. Therefore, we can only conclude that P.ast-7 and O.fav-3a have very low DEVDase activity, which supports our previous data suggesting that these two proteins are inactive monomers in solution. P.ast-3 and O.fav-3b are unexpectedly inactive against Ac-VEID-AFC, the canonical human caspase-6 substrate; O.fav-3b was also inactive against any of the tetra-peptides tested (Table 4.1), but P.ast-3 displayed significant activity against Ac-LEHD-AMC (Fig 4.3).

Table 4.1: Activity Assay Results:  $k_{cat}/K_M$  values ( $M^{-1}s^{-1}$ )

	P.ast-7	P.ast-3	O.fav-3a	O.fav-3b
DEVD-AFC	$5.98 \times 10^4$	n/a	$1.19 \times 10^4$	n/a
VEID-AFC	n/a	n/a	n/a	n/a
LEHD-AMC	n/a	$1.5663 \times 10^3$	n/a	n/a
IETD-AMC	n/a	n/a	n/a	n/a
LETD-AFC	n/a	n/a	n/a	n/a

### 10nM OFAV-3a with DEVD-AFC

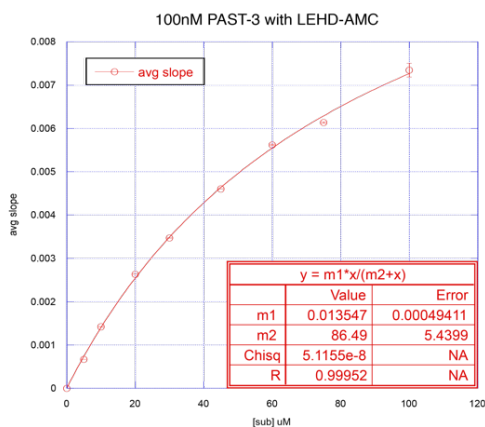
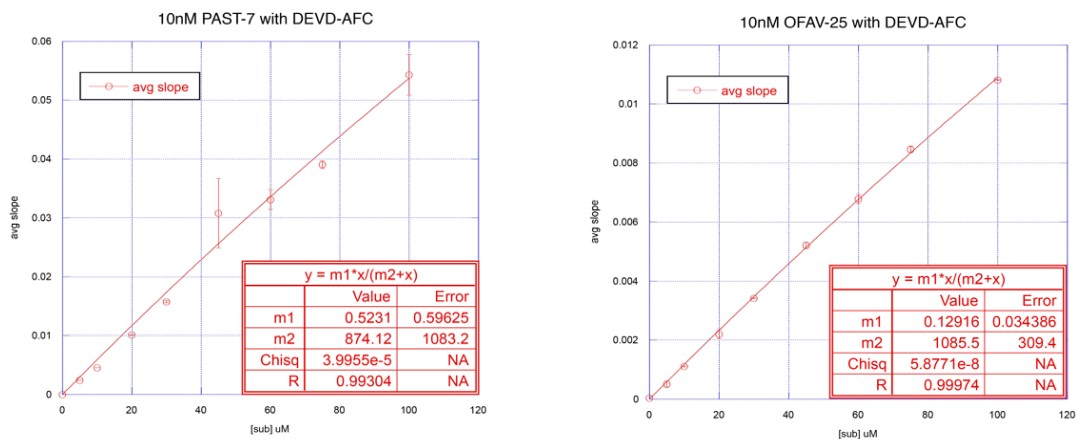


Figure 4.3: Fluorometric Enzyme Assay Data (Michaelis-Menten Curves)

Reaction velocity vs. [sub] in  $\mu\text{M}$

$$k_{\text{cat}} = m1/[\text{enzyme}] \text{ in } \mu\text{M}, K_M \text{ in } \mu\text{M} = m2$$

### 4.3 Resolved Crystal Structure of P.ast-7

P.ast-7 bound with inhibitor DEVD-CHO crystallized in a buffer solution of [0.1 M sodium malonate, 16% PEG 3350, pH 5] (Fig 4.4). These crystals were picked and stored in a cryoprotectant solution: [20% PEG 4000, 80% well solution]. The diffraction data was scaled in HKL-2000, molecular replacement and refinements were done in Phenix, and modelling was done in Coot. The crystal diffracted to 1.57 Å resolution with 98.7% completeness scaled in the P 21 21 21 space group. Other crystallography statistics are



listed in Table 4.2. The resolved structure is shown in Fig 4.5, and the substrate-bound active site and hydrogen bonds are shown in Figs 4.6 and 4.7.

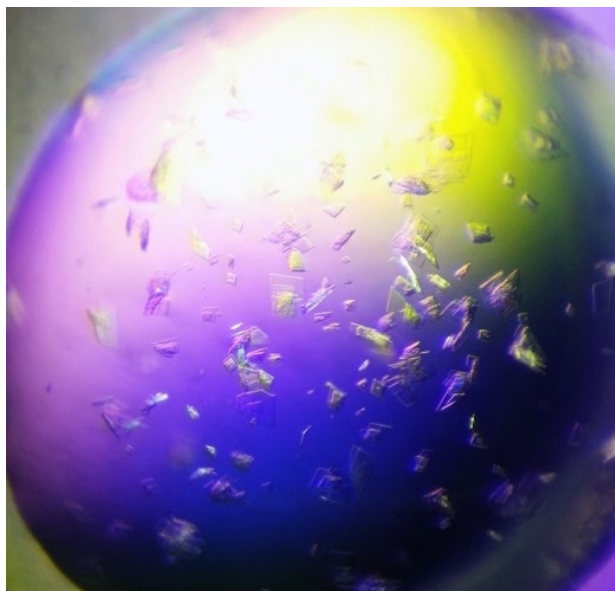
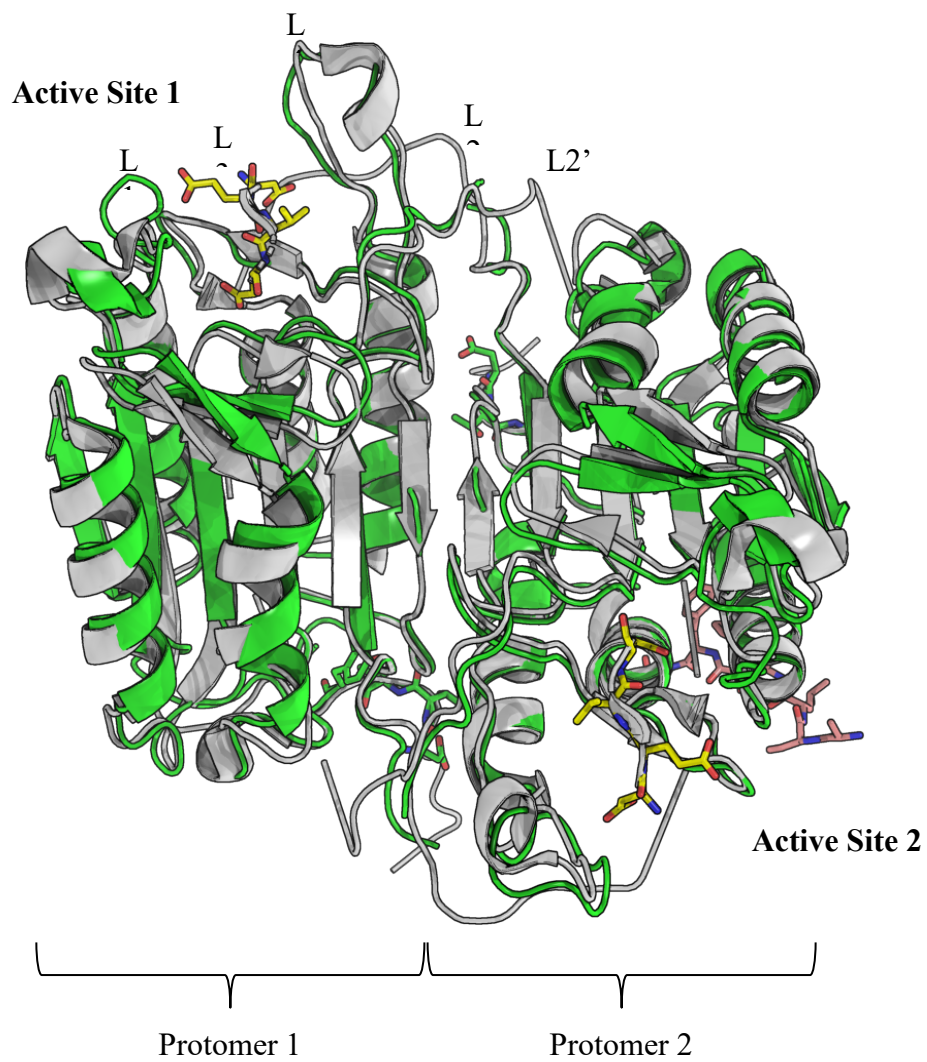


Figure 4.4: Crystallized P.ast-7 + DEVD-CHO

Table 4.2: Crystallography Statistics for Resolved P.ast-7 Structure

Wavelength	1.0	Resolution	39.4 – 1.57
Space Group	P 21 21 21	No. of Reflections	83910
Completeness (%)	98.7	Ramachandran outliers	0.00%
Ramachandran favored	97.86%	Rotamer outliers	0.24%
$\langle I/\sigma(I) \rangle$	1.33	MolProbity score	1.17
$R_{\text{work}}/R_{\text{free}}$ (%)	17.7/20.6	Clashscore	3.51



**Figure 4.5: Resolved P.ast-7 Structure**

P.ast-7 (green) is overlaid with human caspase-3 (gray). Labeled are both individual protomers, both active sites, and loops L1, L2, L2', L3, and L4. In yellow is DEVD-CHO inhibitor. The pink peptide on the right is a bound N-terminal peptide.

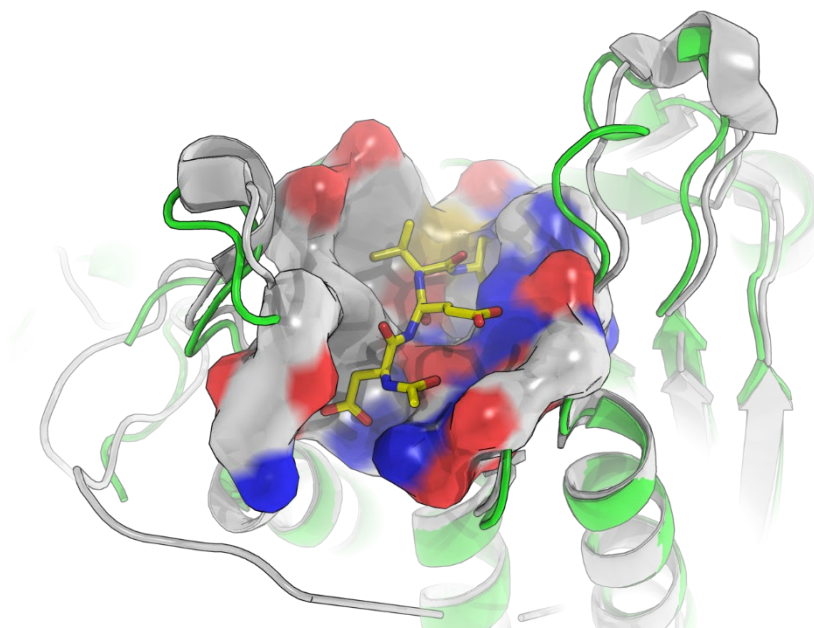


Figure 4.6: P.ast-7 Active Site Bound with DEVD-CHO Inhibitor

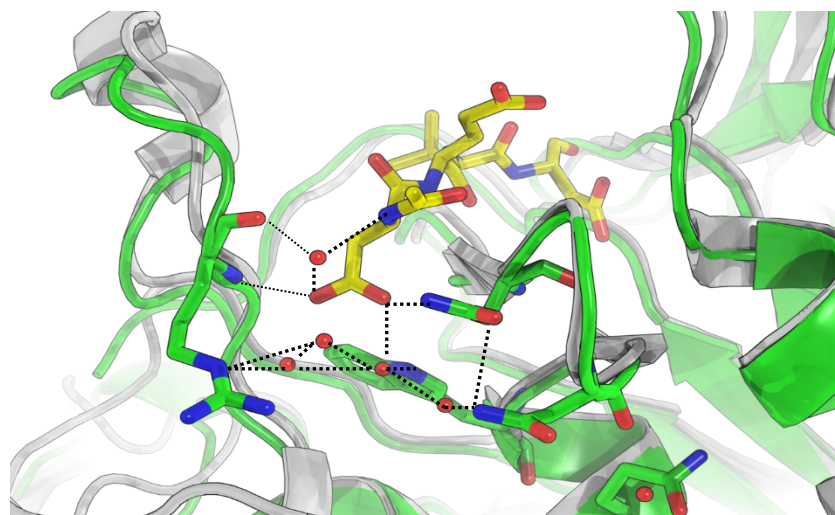


Figure 4.7: Hydrogen-Bonding Network of DEVD in the Active Site

The crystal structure readily reveals two sites of interest near the active site. First, an insertion of RYP (Arg-Tyr-Phe) residues appears to coordinate the substrate in the active site (Fig 4.6); the -COOH group of proline forms hydrogen bonds two water molecules that

interact with the P3 glutamate -COOH side-chain and the P2 valine -COOH group. Secondly, the structure shows that part of the P.ast-7 N-terminus (N'-AKLFSFGG-C') is bound near the active site (Fig 4.5 and Fig 4.7). The P.ast-7 residues immediately following this part of the sequence are not resolved in the structure. Molecular dynamics simulations show that this peptide remains bound with or without inhibitor.

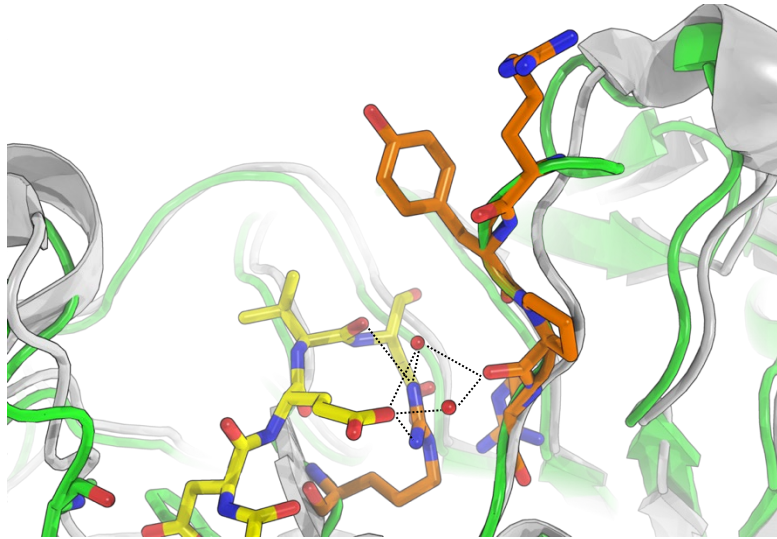


Figure 4.8: Interaction of P.ast-7 RYP Residues with DEVD-CHO

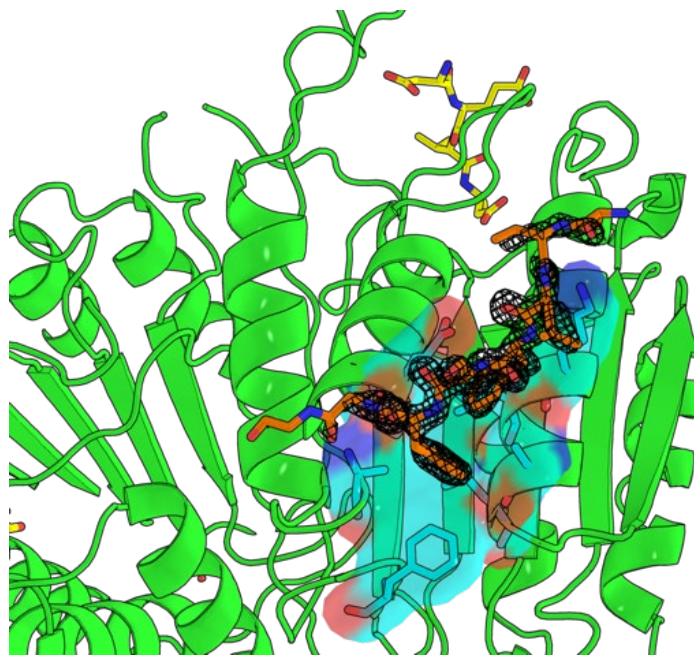


Figure 4.9: Extra N-Terminal Bound Peptide with Electron Density

## CHAPTER 5

### DISCUSSION

Invertebrate caspases were first characterized in *C. elegans* (Ellis & Horvitz, 1986; Yuan & Horvitz, 1990) and *Drosophila* (Song, McCall, & Steller, 1997), but they have proven to be poor models for studying the evolution of the vertebrate apoptotic network. Genomic studies of cnidarians, the sister group to the Bilateria, have found many genes that were previously thought to have been vertebrate innovations. The extensive gene loss in *C. elegans* and *Drosophila* indicate that their apoptotic pathways may not reflect the characteristics of ancestral metazoans (Kortschak et al., 2003). The apoptotic pathway of *C. elegans* involves only one caspase (CED-3) that bears a CARD-domain necessary for its activation (Irmeler, 1997). In contrast, humans have many caspases with discrete functions in the inflammatory and apoptotic pathways (Walsh et al., 2008; Salvesen & Walsh, 2014). Moreover, cytochrome C is not involved in the formation of the apoptosome in *Drosophila*, indicating that this organism lacks the intrinsic pathway found in humans (Dorstyn et al., 2004). The limitations of these model organisms are considerable incentives to study the apoptotic pathways of ancestral groups like the basal metazoans.

Although these coral caspases have high sequence similarity to human executioner caspase-3 and -7, there are many indications that they may be more structurally and functionally similar to other caspases. In fact, P.ast-7 and O.fav-3a share many characteristics of human initiator caspase-2: an inactive monomeric state, presence of the CARD domain, and Group II specificity for DEVD. P.ast-3 and O.fav-3a appear to have a

Group III specificity for valine in the P4 substrate position, but their inactivity against the canonical human executioner caspase-6 substrate VEID suggests that they may possess additional specificities for other positions. The substrate phage display data these two proteins have overwhelmingly selected for phenylalanine and proline in the P3 and P2 positions; such a specificity for bulky and inflexible residues has not been characterized in any vertebrate caspase. Additionally, these two proteins also appear to have a P5 specificity for glutamine; the only human caspase to have a P5 specificity is caspase-2. Another study of Cnidarian caspases found that executioner caspase-3-like proteins in of three species of *Acropora* had initiator caspase-8 specificity (Sakamaki et al., 2014), further demonstrating that sequence similarity is a poor predictor of specificity.

A caspase found in the sea anemone *Aiptasia pallida* has also been reported to share traits of both human initiators and executioners (Dunn et al., 2006). This caspase, described as *acasp* (ancient caspase), appears to have many key characteristics of P.ast-7 and O.fav-3a. All three caspases have primary structures are similar to that of human executioners and they possess CARD domains found only in initiators. Additionally, *acasp* shares the RYP insertion found P.ast-7 and O.fav-3a. The orientation of the amino acids near the P.ast-7 active site suggests its potential function as an auto-inhibitory mechanism, where the side chains of arginine and/or tyrosine rotate and block access to the active site. The hydrogen bonds formed between these residues and the inhibitor also indicate its role in substrate coordination. A crystal structure of O.fav-3a has yet to be obtained, but it is hypothesized that the RYP insertion will have a similar structural presence.

The extra N-terminal peptide bound to P.ast-7 is unusual, and its location near the active site suggests that it may serve as a regulatory exosite—non-catalytic binding sites

that incur additional substrate specificity. At this time, exosite interactions of caspases are not well-studied. We are currently preparing samples of P.ast-7 for mass spectrometry, which will identify cleavage sites in the pro-domain; additionally, we are currently investigating intracellular caspase substrates possessing an upstream DEVD and a downstream hydrophobic sequence that may interact with the bound peptide (Timmer & Salvesen, 2006). In summary, the coral caspases studied here have revealed novel structural features and potential regulatory mechanisms, indicating the complexity of caspase evolution and cnidarian apoptotic pathways.

## REFERENCES

- Boatright, K. M., & Salvesen, G. S. (2003). Mechanisms of caspase activation. *Current Opinion in Cell Biology*, 15(6), 725-731. doi:10.1016/j.ceb.2003.10.009
- Burkepile, D. E., & Hay, M. E. (2008). Coral Reefs. *Encyclopedia of Ecology*, 784-796. doi:10.1016/b978-008045405-4.00323-2
- Burriesci, M. S., Raab, T. K., & Pringle, J. R. (2012). Evidence that glucose is the major transferred metabolite in dinoflagellate-cnidarian symbiosis. *Journal of Experimental Biology*, 215(19), 3467-3477. doi:10.1242/jeb.070946
- Clark, A. C. (2016). Caspase Allosterity and Conformational Selection. *Chemical Reviews*, 116(11), 6666-6706. doi:10.1021/acs.chemrev.5b00540
- De'ath, G., Fabricius, K. E., Sweatman, H., & Puotinen, M. (2012). The 27-year decline of coral cover on the Great Barrier Reef and its causes. *Proceedings of the National Academy of Sciences*, 109(44), 17995-17999. doi:10.1073/pnas.1208909109
- Dorstyn, L., Mills, K., Lazebnik, Y., & Kumar, S. (2004). The two cytochrome *c* species, DC3 and DC4, are not required for caspase activation and apoptosis in *Drosophila* cells. *The Journal of Cell Biology*, 167(3), 405-410. doi:10.1083/jcb.200408054



- Downs, C. A., Fauth, J. E., Halas, J. C., Dustan, P., Bemiss, J., & Woodley, C. M. (2002). Oxidative stress and seasonal coral bleaching. *Free Radical Biology and Medicine*, 33(4), 533-543. doi:10.1016/s0891-5849(02)00907-3
- Dunn, S. R., Phillips, W. S., Spatafora, J. W., Green, D. R., & Weis, V. M. (2006). Highly Conserved Caspase and Bcl-2 Homologues from the Sea Anemone *Aiptasia pallida*: Lower Metazoans as Models for the Study of Apoptosis Evolution. *Journal of Molecular Evolution*, 63(1), 95-107. doi:10.1007/s00239-005-0236-7
- Dunn, S. R., Thomason, J. C., Le Tissier, M., & Bythell, J. C. (2004). Heat stress induces different forms of cell death in sea anemones and their endosymbiotic algae depending on temperature and duration. *Cell Death and Differentiation*, 11(11), 1213-1222. doi:10.1038/sj.cdd.4401484
- Ellis, H. M., & Horvitz, H. R. (1986). Genetic control of programmed cell death in the nematode *C. elegans*. *Cell*, 44(6), 817-829. doi:10.1016/0092-8674(86)90004-8
- Erez, J., Reynaud, S., Silverman, J., Schneider, K., & Allemand, D. (2010). Coral Calcification Under Ocean Acidification and Global Change. *Coral Reefs: An Ecosystem in Transition*, 151-176. doi:10.1007/978-94-007-0114-4\_10
- Frankowiak, K., Wang, X. T., Sigman, D. M., Gothmann, A. M., Kitahara, M. V., Mazur, M., . . . Stolarski, J. (2016). Photosymbiosis and the expansion of shallow-water corals. *Science Advances*, 2(11). doi:10.1126/sciadv.1601122

- Fuess, L. E., C, J. H., Weil, E., Grinshpon, R. D., & Mydlarz, L. D. (2017). Life or death: Disease-tolerant coral species activate autophagy following immune challenge. *Proceedings of the Royal Society B: Biological Sciences*, 284(1856), 20170771. doi:10.1098/rspb.2017.0771
- Grinshpon, R. D. (2018). *Evolutionary Biochemistry of the Caspase: Resurrection of Ancestral Effector Proteases* (Unpublished doctoral dissertation). North Carolina State University.
- Huettenbrenner, S., Maier, S., Leisser, C., Polgar, D., Strasser, S., Grusch, M., & Krupitza, G. (2003). The evolution of cell death programs as prerequisites of multicellularity. *Mutation Research/Reviews in Mutation Research*, 543(3), 235-249. doi:10.1016/s1383-5742(02)00110-2
- Hughes, T. P., Anderson, K. D., Connolly, S. R., Heron, S. F., Kerry, J. T., Lough, J. M., . . . Wilson, S. K. (2018). Spatial and temporal patterns of mass bleaching of corals in the Anthropocene. *Science*, 359(6371), 80-83. doi:10.1126/science.aan8048
- Hughes, T. P., Baird, A. H., Bellwood, D. R., Card, M., Connolly, S. R., Folke, C., . . . Roughgarden, J. (2003). Climate Change, Human Impacts, and the Resilience of Coral Reefs. *Science*, 301(5635), 929-933. doi:10.1126/science.1085046
- Irmeler, M., Hofmann, K., Vaux, D., & Tschopp, J. (1997). Direct physical interaction between the *Caenorhabditis elegans* 'death proteins' CED-3 and CED-4. *FEBS Letters*, 406(1-2), 189-190. doi:10.1016/s0014-5793(97)00271-8

- Jang, T., & Park, H. H. (2013). PIDD mediates and stabilizes the interaction between RAIDD and Caspase-2 for the PIDDosome assembly. *BMB Reports*, 46(9), 471-476. doi:10.5483/bmbrep.2013.46.9.021
- Kerr, J. F., Wyllie, A. H., & Currie, A. R. (1972). Apoptosis: A Basic Biological Phenomenon with Wide-ranging Implications in Tissue Kinetics. *British Journal of Cancer*, 26(4), 239-257. doi:10.1038/bjc.1972.33
- Kortschak, R. D., Samuel, G., Saint, R., & Miller, D. J. (2003). EST Analysis of the Cnidarian *Acropora millepora* Reveals Extensive Gene Loss and Rapid Sequence Divergence in the Model Invertebrates. *Current Biology*, 13(24), 2190-2195. doi:10.1016/j.cub.2003.11.030
- Lemasters, J. J. (2009). Molecular Mechanisms of Cell Death. *Molecular Pathology*, 3-24. doi:10.1016/b978-0-12-374419-7.00001-9
- Lesser, M. P. (1997). Oxidative stress causes coral bleaching during exposure to elevated temperatures. *Coral Reefs*, 16(3), 187-192. doi:10.1007/s003380050073
- Mackenzie, S. H., & Clark, A. C. (2012). Death by Caspase Dimerization. *Advances in Experimental Medicine and Biology Protein Dimerization and Oligomerization in Biology*, 55-73. doi:10.1007/978-1-4614-3229-6\_4
- Mackenzie, S., Schipper, J. L., & Clark, A. C. (2008). The potential for caspases in drug discovery. *Current Cancer Drug Targets*, 8(2), 98-109. doi:10.2174/156800908783769391

- McManus, J. W., Reyes, R. B., Jr., & Nañola, C. L., Jr. (1997). Effects of Some Destructive Fishing Methods on Coral Cover and Potential Rates of Recovery. *Environmental Management*, 21(1), 69-78. doi:10.1007/s002679900006
- Moberg, F., & Folke, C. (1999). Ecological goods and services of coral reef ecosystems. *Ecological Economics*, 29(2), 215-233. doi:10.1016/s0921-8009(99)00009-9
- Nielsen, D. A., Petrou, K., & Gates, R. D. (2018). Coral bleaching from a single cell perspective. *The ISME Journal*, 12(6), 1558-1567. doi:10.1038/s41396-018-0080-6
- Oakley, C. A., & Davy, S. K. (2018). Cell Biology of Coral Bleaching. *Ecological Studies Coral Bleaching*, 189-211. doi:10.1007/978-3-319-75393-5\_8
- Pernice, M., Dunn, S. R., Miard, T., Dufour, S., Dove, S., & Hoegh-Guldberg, O. (2011). Regulation of Apoptotic Mediators Reveals Dynamic Responses to Thermal Stress in the Reef Building Coral *Acropora millepora*. *PLoS ONE*, 6(1). doi:10.1371/journal.pone.0016095
- Ramirez, M. L., & Salvesen, G. S. (2018). A primer on caspase mechanisms. *Seminars in Cell & Developmental Biology*, 82, 79-85. doi:10.1016/j.semcdb.2018.01.002
- Renehan, A. G., Booth, C., & Potten, C. S. (2001). What is apoptosis, and why is it important? *BMJ*, 322(7301), 1536-1538. doi:10.1136/bmj.322.7301.1536

- Richier, S., Sabourault, C., Courtiade, J., Zucchini, N., Allemand, D., & Furla, P. (2006). Oxidative stress and apoptotic events during thermal stress in the symbiotic sea anemone, *Anemonia viridis*. *FEBS Journal*, 273(18), 4186-4198.  
doi:10.1111/j.1742-4658.2006.05414.x
- Riedl, S. J., & Salvesen, G. S. (2007). The apoptosome: Signalling platform of cell death. *Nature Reviews Molecular Cell Biology*, 8(5), 405-413.  
doi:10.1038/nrm2153
- Sakamaki, K., Shimizu, K., Iwata, H., Imai, K., Satou, Y., Funayama, N., . . . Miller, D. J. (2014). The Apoptotic Initiator Caspase-8: Its Functional Ubiquity and Genetic Diversity during Animal Evolution. *Molecular Biology and Evolution*, 31(12), 3282-3301. doi:10.1093/molbev/msu260
- Salvesen, G. S., & Walsh, C. M. (2014). Functions of caspase 8: The identified and the mysterious. *Seminars in Immunology*, 26(3), 246-252.  
doi:10.1016/j.smim.2014.03.005
- Song, Z., McCall, K., & Steller, H. (1997). DCP-1, a *Drosophila* Cell Death Protease Essential for Development. *Science*, 275(5299), 536-540.  
doi:10.1126/science.275.5299.536
- Sutherland, K., Porter, J., & Torres, C. (2004). Disease and immunity in Caribbean and Indo-Pacific zooxanthellate corals. *Marine Ecology Progress Series*, 266, 273-302. doi:10.3354/meps266273

- Tchernov, D., Kvitt, H., Haramaty, L., Bibby, T. S., Gorbunov, M. Y., Rosenfeld, H., & Falkowski, P. G. (2011). Apoptosis and the selective survival of host animals following thermal bleaching in zooxanthellate corals. *Proceedings of the National Academy of Sciences*, *108*(24), 9905-9909. doi:10.1073/pnas.1106924108
- Thurber, R. L., Burkepile, D. E., Fuchs, C., Shantz, A. A., Mcminds, R., & Zaneveld, J. R. (2013). Chronic nutrient enrichment increases prevalence and severity of coral disease and bleaching. *Global Change Biology*, *20*(2), 544-554. doi:10.1111/gcb.12450
- Timmer, J. C., & Salvesen, G. S. (2006). Caspase substrates. *Cell Death and Differentiation*, *14*(1), 66-72. doi:10.1038/sj.cdd.4402059
- Tinel, A. (2004). The PIDDosome, a Protein Complex Implicated in Activation of Caspase-2 in Response to Genotoxic Stress. *Science*, *304*(5672), 843-846. doi:10.1126/science.1095432
- Tjus, S. E., Scheller, H. V., Andersson, B., & Moller, B. L. (2001). Active Oxygen Produced during Selective Excitation of Photosystem I Is Damaging Not Only to Photosystem I, But Also to Photosystem II. *Plant Physiology*, *125*(4), 2007-2015. doi:10.1104/pp.125.4.2007
- Walsh, J. G., Cullen, S. P., Sheridan, C., Luthi, A. U., Gerner, C., & Martin, S. J. (2008). Executioner caspase-3 and caspase-7 are functionally distinct proteases. *Proceedings of the National Academy of Sciences*, *105*(35), 12815-12819. doi:10.1073/pnas.0707715105

- Warner, M. E., Fitt, W. K., & Schmidt, G. W. (1999). Damage to photosystem II in symbiotic dinoflagellates: A determinant of coral bleaching. *Proceedings of the National Academy of Sciences*, 96(14), 8007-8012. doi:10.1073/pnas.96.14.8007
- Wei, M. C., Zong, W. X., Cheng, E. H., Lindsten, T., Panoutsakopoulou, V., Ross, A. J., . . . Korsmeyer, S. J. (2001). Proapoptotic BAX and BAK: A Requisite Gateway to Mitochondrial Dysfunction and Death. *Science*, 292(5517), 727-730. doi:10.1126/science.1059108
- Wiens, M., Krasko, A., Perovic, S., & Müller, W. E. (2003). Caspase-mediated apoptosis in sponges: Cloning and function of the phylogenetic oldest apoptotic proteases from Metazoa. *Biochimica Et Biophysica Acta (BBA) - Molecular Cell Research*, 1593(2-3), 179-189. doi:10.1016/s0167-4889(02)00388-9
- Yu, X., Huang, B., Zhou, Z., Tang, J., & Yu, Y. (2017). Involvement of caspase3 in the acute stress response to high temperature and elevated ammonium in stony coral *Pocillopora damicornis*. *Gene*, 637, 108-114. doi:10.1016/j.gene.2017.09.040
- Yuan, J., & Horvitz, H. (1990). The *Caenorhabditis elegans* genes *ced-3* and *ced-4* act cell autonomously to cause programmed cell death. *Developmental Biology*, 138(1), 33-41. doi:10.1016/0012-1606(90)90174-h

## BIOGRAPHICAL INFORMATION

Jessica Tung was born and raised in Bloomington-Normal, Illinois. After a brief stint as a professional clarinetist in the DFW area, she returned to academia with interest in applying to medical school upon graduation. However, she did not anticipate discovering an aptitude and passion for scientific inquiry while working as an undergraduate researcher in the biochemistry lab of Dr. Clay Clark. In Dr. Clark's lab, Jessica, alongside a graduate student, studied the evolutionary trajectories of apoptotic caspases via ancestral state reconstruction. After gaining independence as a researcher, she received a grant from the UTA Undergraduate Research Opportunity Program to investigate the structural biochemistry of four novel coral caspases. Her work has resulted in both a poster presentation at the 32nd Annual Gibbs Conference on Biological Thermodynamics and a forthcoming publication. She graduated with Spring 2019 with an Honors Bachelor of Science in Biology and minor in biochemistry. Moving forward, Jessica aspires to pursue a dual M.D./Ph.D. degree and conduct biomedical research at either a university or in a government capacity.